Singularity Analysis with respect to the Workspace of a Double Parallel Manipulator

Lee, Min Ki and Park, Kun Woo*

(*Received July 5, 1998*)

Singularity analysis is an important issue in the design of parallel manipulators, since they become uncontrollable at singular configurations due to the rank deficiency of the Jacobian. This paper analyzes the singularity of a double parallel manipulator with respect to its workspace. The workspace is decoupled into a positional workspace generated by the first parallel mechanism, and an orientational workspace by the second mechanism. The singularities occurring outside each workspace are analytically found by a Jacobian matrix derived for the velocity transformation from the end-effecfor to the linear actuators. The singularity loci are presented and their geometric properties are examined to prove that the double parallel manipulator is free from the singularity problem.

Key Words: Double Parallel Mechanism, Singular Configuration, Positional and Orientational Workspace

1. Introduction

In comparison with serial manipulators, parallel manipulators have several advantages such as load-carrying capacity, stiffness, and mechanical inertia (Kerr, 1989). However, it has a smaller workspace (Gosselin, 1990) and greater complexity in the kinematics and dynamics (Sugimoto, 1987), which has motivated us to design a Double Parallel Manipulator (Lee, 1995) (DPM) by stacking two Parallel Mechanisms (PMs) vertically. The DPM achieves simplicity in the kinematics and dynamics by decoupling the motion of each PM, and it has a large workspace by reducing the number of linear actuators in each platform to avoid link interference (Lee and Park, 1997). However, Kinematic singularity, which is an important issue in mechenism design, has not been examined yet.

The singularities encountered in kinematic chains can be divided into three main groups (Gosselin and Angeles, 1990). The first kind of singularity occurs when the output link loses one or more degrees of freedom, and the second kind of singularity arises at configurations where the output link is locally movable even when all the actuated joints are locked. The third kind of singularity is of a slightly different nature than the first two since it requires conditions on the linkage parameters. This corresponds to configurations in which the chain can undergo finite motions when its actuators are locked.

Singularities are analyzed by the configurations at which the Jacobian determinants become zero (Gosselin, Perreault and Vaillancourt, 1995). This is a laborious procedure that leads to inconclusive results in the PM since the singularities cannot be confined to a specific region and also cannot be easily geometrically ascertained due to the Jacobian matrix's functional complexity. Fichter (Fichter, 1986) studied the singular configurations of a Stewart Platform, While Long and Collins (Long and Collins, 1995) geometrically analyzed singularities by line vectors involved in three pantograph linkages. However, they have not examined the relationship between singularities and the workspace, which is a more practical issue for avoiding singularities.

* Dept. of Control and Instrumentation Engr. Changwon National Univ.

This paper investigates singularity regions with respect to the workspace to prove that singularities of the DPM occur outside the workspace.

2. Structure of the DPM

The DPM is made up of two PMs with a central axis as shown in Fig. 1. In the first PM, for i=1, 2, 3, linear actuators LA_i are connected from Bi of Base-1 to Pi of Platform-1 through universal joints placed for $\|\overrightarrow{O_{B_1}B_i}\|=r_{B1}$ and $\|\overrightarrow{O_{P_1}P_i}\|=r_{P1}$. B_1 and B_2 are symmetrically located for $\angle B_{i(i=1,2)}O_{B_1}B_3=\zeta_{B1}$, and P_1 and P_2 are also symmetric for $\angle P_{i(i=1,2)}O_{P_1}P_3=\zeta_{P1}$. Similarly, for i=4, 5, LA_i of the second PM are connected from Bi of Base-2 to Pi of Platform-2, which are located for $\|\overrightarrow{O_{B_2}B_i}\|=r_{B2}$ and $\|\overrightarrow{O_{P_2}P_i}\|=r_{P2}$, forming angles ζ_{B2} and ζ_{P2} from the horizontal axis. O_{Bi} (i=1, 2) and O_{P_i} (i=1, 2) are the center points of the bases and platforms, respectively. As viewed in Fig. 2, the link train of LA_i is composed of θ_{i1}-θ_{i2}-θ_{i3}-θ_{i4}-θ_{i5}-θ_{i6}, which are all passive joints except for the sliding joint θ_{i3} whice is actively actuated to vary the length of LA_i. To increase the rotational range of the universal joints, offset links are inserted in the upper universal joints of the first PM and in the lower joints of the second PM.

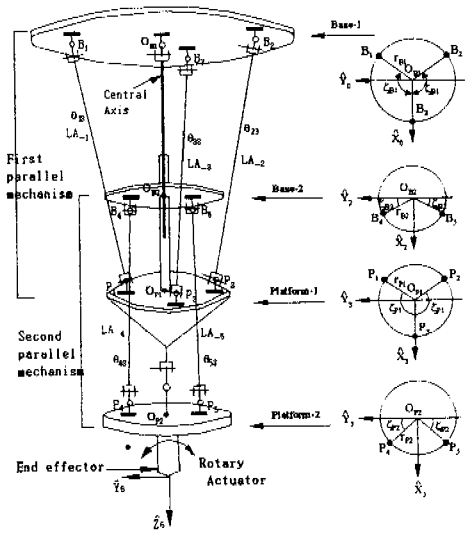

Fig. 1 Double parallel manipulator.

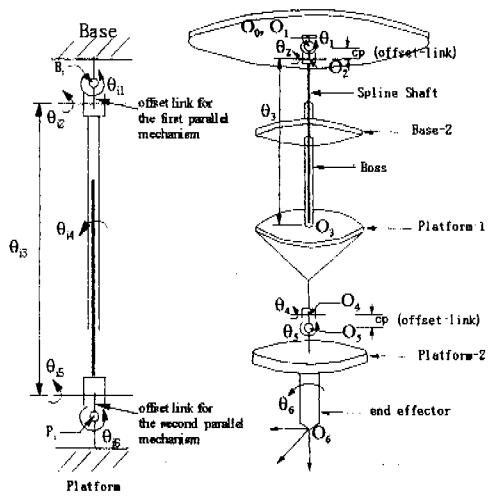

Fig. 2 Linear actuator and central axis.

A central axis is comprised of all passive joints θ_1-θ_2-θ_3-θ_4-θ_5 with offset links inserted in both the upper and lower universal joints. While θ_1-θ_2-θ_3 places platform-1 at a desired position by constraining the first PM, θ_4-θ_5 rotate the platform-2 to a desired orientation using the second PM. It is important to note the passive joint displacements θ_1-θ_2-θ_3 and θ_4-θ_5 are decoupled and independently generated by LA_i(i=1, 2, 3) and LA_i(i=4, 5), respectively. Therefore the orientational workspace of the second PM is geometrically decoupled from the positional workspace of the first PM. Adding θ_6 to the second PM provides the DPM with 6-degrees of freedom. For kinematic analysis, Cartesian coordinates {i} (i=0,…, 6) are assigned to joints of the central axis as viewed in Figs. 1 and 2.

3. Workspace Analysis

Many researchers (Fichter, 1986; Waldron, Raghavan and Roth, 1989) depicted the reachable workspace of a platform using inverse kinematics. Gosselin (Gosselin, 1990) analytically computed the workspace volume by dissecting it into sectional areas to be integrated. The previous works focus on the positional workspace which a platform is able to reach with a fixed orientation. In practice, a workspace with the small range of possible orientations is generally not useful. Hence the orientational workspace must be

Table 1. Design parameters of DPM.

Name	$\theta_{3\ \min}$	$\theta_{3\ \max}$	Name	
central axis	743	1133	r_{B1}	250
			r_{P1}	120
Name	$\theta_{i3\ \min}$	$\theta_{i3\ \max}$	r_{B2}	80
			r_{P2}	150
LA_i (i=1,2,3)	754	1140	$l=\lvert\overrightarrow{O_{B2}O_4}\rvert$	730
			cp	20
LA_i (i=4,5)	630	835	$\zeta_{Bi(i=1,2)}$	120°, 20°
			$\zeta_{Pi(i=1,2)}$	120°, 45°

examined. This paper presents a positional and an orientational workspace separately, and analyzes singularity loci occurring in each space. Using the interference decision algorithms derived by Merlet (Merlet, 1994), we determine the design parameters indicated in Table I to maximize the workspace avoiding interference.

It is noted that offset links enlarge the rotational range of universal joints but their short lengths yield little influence on the workspace and singularities. Hence we neglect them but keep the wide range from the offset links. The range of universal joints with an offset link is 70°, but the range without offset links is reduced to 25° due to yoke interference. For a well-designed DPM, there is no interference within the ranges of the linear actuators. Thus the workspace is obtained by comb ining the space generated by the linear actuators moving from the minimum to the maximum length.

The position of Platform-1 attained by LA_i(i =1, 2, 3) is computed for a positional workspace which is described as $\overrightarrow{{}^0O_{B_1}O_{P_1}}$. From closed loops $O_{B_1}B_iP_iO_{P1}O_{B_1}$, the length of LA_i are

$$\theta_{i3}=\|\overrightarrow{{}^0O_{B_1}O_{P_1}}-\overrightarrow{{}^0O_{B_1}B_i}+{}^0R_3\overrightarrow{{}^3O_{P_1}P_i}\| \quad (1)$$

where the superscripts represent the coordinates describing vectors and matrices. Let $\{x, y, z\}^T=\overrightarrow{{}^0O_{B_1}O_{P_1}}$ and $\{x_{0i}, y_{0i}, z_{0i}\}^T=\overrightarrow{{}^0O_{B_1}B_i}-{}^0R_3\overrightarrow{{}^3O_{P_1}P_i}$ θ_{i3}^2 of Eq. (1) is written as

$$\theta_{i3}^2=(x-x_{0i})^2+(y-y_{0i})^2+(z-z_{0i})^2 \quad (i=1, 2, 3) \quad (2)$$

With $\overrightarrow{{}^0O_{B_1}B_i}=\{x_{Bi}, y_{Bi}, z_{Bi}\}^T$ and $\overrightarrow{{}^3O_{P_1}P_i}=\{x_{pi}, y_{pi}, z_{pi}\}^T$ x_{0i}, y_{0i} and z_{0i} are described by

$$\begin{aligned} x_{0i}&=x_{Bi}-r_{11}x_{Pi}-r_{12}y_{Pi}-r_{13}z_{Pi}\\ y_{0i}&=y_{Bi}-r_{12}x_{Pi}-r_{22}y_{Pi}-r_{23}z_{Pi}\\ z_{0i}&=z_{Bi}-r_{31}x_{Pi}-r_{32}y_{Pi}-r_{33}z_{Pi} \end{aligned} \quad (3)$$

where r_{ij} are elements of ${}^0R_3$ expressed by θ_1, θ_2 and θ_3 Forward kinematics of the central axis yields

$$\begin{aligned} &x=\theta_3 s(\theta_2),\quad y=-\theta_3 s(\theta_1)c(\theta_2),\\ &z=\theta_3 c(\theta_1)c(\theta_2) \end{aligned} \quad (4)$$

where $s(.)=\sin(.)$ and $c(.)=\cos(.)$. Solving for θ_1, θ_2 and θ_3 with x, y and z and substituting them into ${}^0R_3$ gives

$${}^0R_3=\begin{bmatrix} \frac{\sqrt{y^2+z^2}}{\sqrt{x^2+y^2+z^2}} & 0 & \frac{x}{\sqrt{x^2+y^2+z^2}} \\ \frac{-xy}{\sqrt{x^2+y^2+z^2}\sqrt{y^2+z^2}} & \frac{z}{\sqrt{y^2+z^2}} & \frac{y}{\sqrt{x^2+y^2+z^2}} \\ \frac{-xz}{\sqrt{x^2+y^2+z^2}\sqrt{y^2+z^2}} & \frac{-y}{\sqrt{y^2+z^2}} & \frac{z}{\sqrt{x^2+y^2+z^2}} \end{bmatrix} \quad (5)$$

All elements are expressed by a unique solution at $-\frac{\pi}{2}<\theta_i(i=1, 2)<\frac{\pi}{2}$, which is always true because the range of the universal joints should not be beyond $\pm\frac{\pi}{2}$. For $l_{i\ \min}\le\theta_{i3}\le l_{i\ \min}$, Eq. (2) with minimum and maximum lengths is respectively rewritten as

$$l_{i\ \min}^2=(x-x_{0i})^2+(y-y_{0i})^2+(z-z_{0i})^2 \quad (i=1, 2, 3) \quad (6a)$$

$$l_{i\ \max}^2=(x-x_{0i})^2+(y-y_{0i})^2+(z-z_{0i})^2 \quad (i=1, 2, 3) \quad (6b)$$

The equations represent the spheres where radii are $l_{i\ \min}^2$ and $l_{i\ \max}^2$, respectively, with changing centers $\{x_{0i}, y_{0i}, z_{0i}\}$. For i=1, 2, 3, the workspace is confined to the space betwean an inner sphere with radius $l_{i\ \min}$ and an outer sphere with radius $l_{i\ \max}$. Fixing $z=z_k$ in Eqs(6a) and (6b), we obtain

$$R_{i\ \min}^2=(x-x_{0i})^2+(y-y_{0i})^2 (i=1, 2, 3) \quad (7a)$$

$$R_{i\ \max}^2=(x-x_{0i})^2+(y-y_{0i})^2 (i=1, 2, 3) \quad (7b)$$

where

$$R_{i\ \min}^2=\begin{cases} l_{i\ \min}^2-(z_k-z_{0i})^2 & \text{for } l_{i\ \min}^2-(z_k-z_{0i})^2>0 \\ 0 & \text{for } l_{i\ \min}^2-(z_k-z_{0i})^2\le 0 \end{cases}$$

$$R_{i\ \max}^2=\begin{cases} l_{i\ \max}^2-(z_k-z_{0i})^2 & \text{for } l_{i\ \max}^2-(z_k-z_{0i})^2>0 \\ 0 & \text{for } l_{i\ \max}^2-(z_k-z_{0i})^2\le 0 \end{cases}$$

These describe circles where radii are $R_{i\,\min}$ and $R_{i\,\max}$, respectively, with changing centers $\{x_{0i}, y_{0i}\}$ yielding ellipsoidal curves. These cause complications in the workspace analysis of the DPM. For the Stewart Platform workspace expressed by Gosselin (Gosselin, 1990), the centers are fixed for circles so that the arcs surrounding the sectional areas are easily found. But the arcs with changing centers must be detected by the roots of the constraint eqs (7a) and (7b). Closed curves formed by the roots x and y are found from

$$S_{i\,\min}=f_{i\,\min}(x, y) \text{ for } R_{i\,\min}(i=1, 2, 3) \quad (8a)$$

$$S_{i\,\max}=f_{i\,\max}(x, y) \text{ for } R_{i\,\max}(i=1, 2, 3) \quad (8b)$$

For each linear actuator, $f_{i\,\min}$ and $f_{i\,\max}$ are functions of $S_{i\,\min}$ and $S_{i\,\max}$, respectively, representing an annular area $A_{i\,zk}$. Due to the distance of the linear actuators, an actuator restricts the regions generated by the others. Hence the workspace is the common region in which all three annular areas are included:

$$A_{zk}=A_{1\,zk}\cap A_{2\,zk}\cap A_{3\,zk} \quad (9)$$

To compute A_{zk} surrounded by several arcs, we sort the inner and outer boundary arcs with intersecting points and then apply the Gauss Divergence Tbeibar(Kreyszig, 1982) to compute the area.:

$$A_i=1/2\int_{S_i} Q_i \cdot n_i dS_i \quad (10)$$

where Q_i is a distance vector from the origin to dS_i and n_i is a normal vector to dS_i. Since n_i has negative or positive directions according to the boundaries, A_{zk} is obtained by subtracting the area enclosed by the inner boundary from the area enclosed by the outer boundary. Summing the sectional areas multiplied by height h_k yields the volume of the workspace:

$$W_{pos}=\sum_{k=0}^{M} A_{zk}\, h_k \quad (11)$$

Figure 3 depicts the sectional areas of the positional workspace at z_h=730, 900, and 1100. At small heights (z_h=730), the annular area$A_{i\,zk}$ surrounded by $S_{i\,\min}$ and $S_{i\,\max}$ occur because both $l_{i\,\min}$ and $l_{i\,\max}$ restrict the workspace, but at large heights (z_h=900, 1100) $S_{i\,\min}$ disappears due to no restriction by $l_{i\,\max}$. A large area is

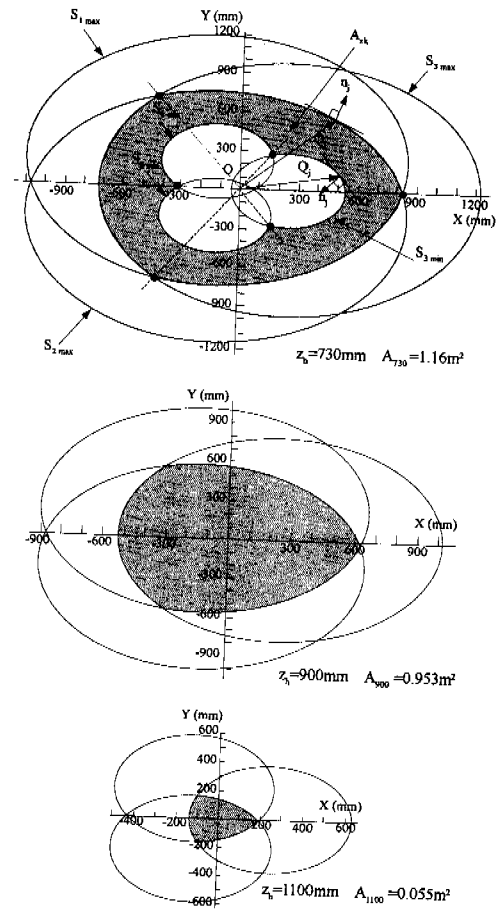

Fig. 3 Positional workspace of DPM in X-Y plane at z_h=730, 900 and 1100.

acquired at small heights but there is an unreachable interior region which is the useful space. Hence we sum the sectional areas from z_h= 800mm to z_h=1132mm to get 0.228m³ for a positional workspace with reachable interior region.

Next, we analyze the orientational workspace expressed by θ_4 and θ_5 which are the rotated angles of platform-2 with respect to base-2. From the closed loops $O_{P_2}O_{B_2}B_iP_iO_{P_2}$ for i=4, 5, the length of LA_i is

$$\theta_{i3}=\|\overrightarrow{{}^5O_{P_2}O_{B_2}}-\overrightarrow{{}^5O_{P_2}P_i}+{}^5R_2\overrightarrow{{}^2O_{B_2}B_i}\| \quad (12)$$

where

$${}^5R_2=\begin{bmatrix} c(\theta_4) & s(\theta_4)s(\theta_5) & s(\theta_4)c(\theta_5) \\ 0 & c(\theta_5) & -s(\theta_5) \\ -s(\theta_4) & c(\theta_4)s(\theta_5) & c(\theta_4)c(\theta_5) \end{bmatrix},$$

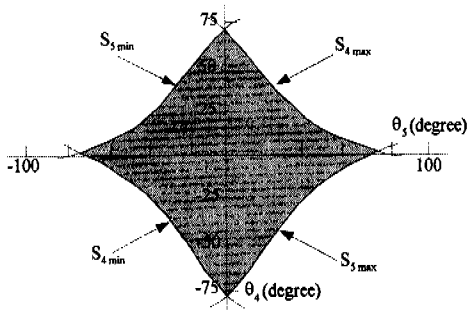

Fig. 4 Orientational workspace of DPM.

$\overrightarrow{{}^5O_{P_2}O_{B_2}}=\{ls(\theta_4)c(\theta_5),\ -ls(\theta_5),\ lc(\theta_4)c(\theta_5)\}$

and l is the fixed distance from O_4 to O_{B_2}. Substituting the minimum and maximum lengths into Eq. (12) yields

$$l_{i\max}^2=\|\overrightarrow{{}^5O_{P_2}O_{B_2}}-\overrightarrow{{}^5O_{P_2}P_i}+{}^5R_2\overrightarrow{{}^2O_{B_2}B_i}\|^2 \quad (13a)$$

$$l_{i\min}^2=\|\overrightarrow{{}^5O_{P_2}O_{B_2}}-\overrightarrow{{}^5O_{P_2}P_i}+{}^5R_2\overrightarrow{{}^2O_{B_2}B_i}\|^2 \quad (13b)$$

Curves formed by the roots θ_4 and θ_5 of the above equations are

$$S_{i\min}=f_{i\min}(\theta_4,\ \theta_5) \quad (14a)$$

$$S_{i\max}=f_{i\max}(\theta_4,\ \theta_5) \quad (14b)$$

The common region bounded by $S_{i\min}$ and $S_{i\max}$ is the orientational workspace:

$$W_{ori}=A_4\cap A_5 \quad (15)$$

Figure 4 shows the orientational workspace surrounded by $S_{i\min}$ and $S_{i\max}$ for i=4, 5. The ranges of θ_4 and θ_5 are $\pm 75°$, respectively, which is independently generated by LA_i(i=4, 5) and decoupled from the positional workspace.

4. Singularity Analysis

For a Stewart Platform, the Jacobian can be derived using screw theory (Fichter, 1986). Howevers a it cannot be directly applied to the DPM since velocities are separately generated in the first and the second PM. Instead, we use a motor (Sugimoto, 1987) defined by the relationship between the velocity of a joint and the resultant velocity of the platform. If the velocity of point "o" in the platform is $\{V_p\ \Omega_p\}^T$ generated by a unit velocity of joint θ_{ij}, then a 6×1 motor vector is defined as ${}^oM_{ij}=\{V_p,\ \Omega_p\}^T$. The left superscript indicates the point where the velocities are inspected and the right subscripts i and j represent the numbers for the link train and joint, respectively.

From the definition of motor, the velocity of an end effector is

$$Vel\_O_6=\dot{\theta}_1{}^{O_6}M_{c1}+\dot{\theta}_2{}^{O_6}M_{c2}+\cdots+\dot{\theta}_6{}^{O_6}M_{c6} \quad (16)$$

where Vel_O_6, which is a 6x1 vector, represents the linear and angular velocity of a point O_6 assigned to the end effector. ${}^{O_6}M_{ci}$ is the motor of joint i of the central axis and $\dot{\theta}_i$ is the joint velocity. Let ${}^{O_6}J_c=[{}^{O_6}M_{c1}\ {}^{O_6}M_{c2}\cdots{}^{O_6}M_{c6}]$; the joint velocities of a central axis are the

$$\dot{\Theta}={}^{O_6}J_c^{-1}\ Vel\_O_6 \quad (17)$$

where $\dot{\Theta}=[\dot{\theta}_1,\ \dot{\theta}_2,\ \cdots,\ \dot{\theta}_6]^T$. Only velocity $\dot{\theta}_6$ is directly controlled by an active joint but the other passive velocities $\dot{\theta}_i$(i=1, 2, ···, 5) must be indirectly generated by LA_i (i=1, 2, ···, 5). To compute the linear actuator velocity, we analyze the velocities of platform-1 and -2. Due to the short length of the offset links, they do not affect the velocities much but increase complexity by including revolute velocities. Thus we neglect the offset links. From the joint velocities and the motors of the central axis, the linear velocities of point Pi, $[Vel\_P_i]_V$, with respect to base-1 and base-2 are obtained respectively by

$$[Vel\_P_i]_V=\dot{\theta}_1[{}^{p_i}M_{c1}]_V+\dot{\theta}_2[{}^{p_i}M_{c2}]_V\ \dot{\theta}_3[{}^{p_i}M_{c3}]\ (i=1,\ 2,\ 3) \quad (18)$$

$$[Vel\_P_i]_V=\dot{\theta}_4[{}^{p_i}M_{c4}]_V+\dot{\theta}_5[{}^{p_i}M_{c5}]_V\ (i=4,\ 5) \quad (19)$$

where a 3×1 vector, $[.]_V$, is the linear velocity component of motor [.]. Ignoring the offset link, $[Vel\_P_i]_V$ can be projected to the velocity of linear actuator:

$$\dot{\theta}_{i3}=u_i^T[Vel\_P_i]_V \quad (20)$$

where u_i is the unit vector of linear actuator, which is obtained from

$$u_i=[u_{ix}\ u_{iy}\ u_{iz}]^T=\frac{\overrightarrow{B_iP_i}}{\|\overrightarrow{B_iP_i}\|} \quad (21)$$

Let us define the following matrices formed by the motors:

$$[{}^{p_i}J_c]_V[[{}^{p_i}M_{c1}]_V\ [{}^{p_i}M_{c2}]_V\ [{}^{p_i}M_{c3}]_V]\ (i=1,\ 2,\ 3) \quad (22)$$

$$[{}^{p_i}J_c]_V[[{}^{p_i}M_{c4}]_V\ [{}^{p_i}M_{c5}]_V]\ (i=4,\ 5) \quad (23)$$

and combine Eqs (17) to (23) to yield

$$[\dot{\theta}_{13}\ \dot{\theta}_{23}\ \dot{\theta}_{33}\ \dot{\theta}_{43}\ \dot{\theta}_{53}\ \dot{\theta}_{6}]^T = A_s B_s {}^{O_6}J_c^{-1}\ Vel\_O_6 \tag{24}$$

where A_s and B_s are 6×16 and 16×6 matrices, respectively, written as

$$A_s = \begin{bmatrix} u_1^T & & & & & & \\ & u_2^T & & & & 0 & \\ & & u_3^T & & & & \\ & & & u_4^T & & & \\ & & & & u_5^T & & \\ & 0 & & & & u_5^T & \\ & & & & & & 1 \end{bmatrix},$$

$$B_s = \left[\begin{array}{ccc} [{}^{p_1}J_c]_V & & \\ [{}^{p_2}J_c]_V & 0_{(9\times3)} & \\ [{}^{p_3}J_c]_V & & \\ \hline & [{}^{p_4}J_c]_V & 0_{(3\times1)} \\ 0_{(7\times3)} & [{}^{p_5}J_c]_V & 0_{(3\times1)} \\ \hline & 0_{(1\times2)} & 1 \end{array}\right]$$

Therefore, the Jacobian matrix relating Vel_O_6 to the linear actuator velocities is

$$J_s = A_s B_s {}^{O_6}J_c^{-1} \tag{25}$$

The Jacobian determinant is

$$Det[J_s] = Det[A_s B_s]\ Det[{}^{O_6}J_c^{-1}] \tag{26}$$

For the singularity analysis of a central axis, we use $Det[{}^{O_6}J_c]$ rather than $Det[{}^{O_6}J_c^{-1}]$ since the singularity occurs even though $Det[{}^{O_6}J_c]=0$, which is simply expressed by

$$Det[{}^{O_6}J_c] = -\theta_3^2\ c(\theta_2)\ c(\theta_5) \tag{27}$$

This involves only three joint displacements θ_i (i=2, 3, 5) not causing $Det[{}^{O_6}J_c]=0$ due to $\theta_3>0$ and $-90°<\theta_i$(i=2, 5)$<90°$, which are always true because θ_3 is the length and θ_i (i=2, 5) are the angles of universal joints. Therefore, no singularity arises from the central axis.

Next, to examine the singularity of the PMs, $Det[A_s B_s]$ is divided by θ_{i3}:

$$Det[{}^sAB] = Det[A_s B_s]/\theta_{i3} \tag{28}$$

Partitioning ${}^sAB$ to 4 sub-matrices yields

$${}^sAB = \begin{bmatrix} FD_{(3\times3)} & 0_{(3\times3)} \\ 0_{(3\times3)} & SD_{(3\times3)} \end{bmatrix}$$

As shown, the determinant is decoupled by

$$Det[{}^sAB] = Det[FD]\ Det[SD] \tag{29}$$

where $Det[FD]$ and $Det[SD]$ are the determinants of the first and the second PMs, respectively, written as Eqs. (30) and (31).

The first PM singularity is determined by three variables θ_i(j=1, 2, 3) for $Det[FD]=0$, Fig. 5 shows the singularity loci σ_i(i=1, 2) at $\theta_3=$ 900mm. Although θ_3 is varied from 800mm to 1100mm, the deviations of θ_1 and θ_2 are less than $\pm1°$. This indicates that the loci are not influenced much by θ_3. σ_1 reveals the cases in which $\theta_1\fallingdotseq 0°$ and $\theta_2\fallingdotseq 90°$ while σ_2 shows the configurations at which LA_i(i=1, 2, 3) are close to the plane of the Base-1 by combining θ_1 and θ_2 to 90°. From

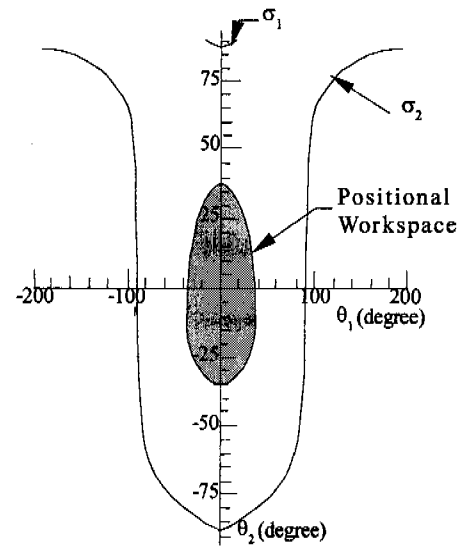

Fig. 5 The singularity loci of the first PM.

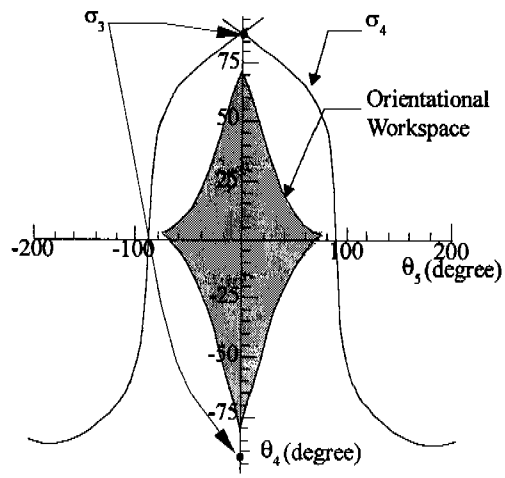

Fig. 6 The singularity loci of the second PM.

these results, it is found that the singularities in the first PM never occur inside the regular workspace.

As shown in Fig. 6, the second PM singularity loci σ_i(i=3, 4) are found by two roots θ_4 and θ_5 for $Det[SD]=0$. When the directions of LA_i (i =4, 5) are collinear on platform-2, singularities arise because velocity transformations cannot be accomplished. In reality, such configur ations do not arise since θ_4 is close to $\pm 90°$, causing linear actuators to contact platform-2. These singularities are depicted by two points of σ_3. When platform-2 is rotated to 90° by combining θ_4 and θ_5, the singularity locus σ_4 arises. Like the first PM, these singularity loci never occur in the regular workspace. Therefore all loci σ_i(i=1, 2, 3, 4) are outside the positional and the orientational workspaces presented in Figs. 3 and 4. This show that the DPM is free from the singularity problem within the regular workspace.

$$Det[FD]=\frac{r_{B1}^2 c(\zeta_{B1})}{32}\begin{bmatrix} 32\theta_3 r_{B1} r_{P1} c(\zeta_{B1}) c(\zeta_{P1}) \\ -12\theta_3 r_{P1}^2+48\theta_3^3 \\ 6\theta_3 r_{P1}^2+24\theta_3^3 \\ 6\theta_3 r_{B1} r_{P1} \\ 8\theta_3 r_{P1}^2 \zeta_{B1} c(\zeta_{P1}) \\ 16\theta_3^2 r_{P1} c(\zeta_{B1}) c(\zeta_{P1}) \\ 12_{B1} r_{P1}^2 c(\zeta_{B1}) c(\zeta_{P1}) \\ 3 r_{B1} r_{P1}^2 \end{bmatrix}^T \begin{bmatrix} -1+c(2\theta_1) \\ c(\theta_1) \\ c(\theta_1-2\theta_2)+c(\theta_1+2\theta_2) \\ -c(\theta_1-\theta_2)-c(\theta_1+\theta_2)+c(\theta_1-3\theta_2)+c(\theta_1+3\theta_2) \\ -2c(\theta_2)+c(2\theta_1-\theta_2)+c(2\theta_1+\theta_2) \\ 2s(\theta_2)+s(2\theta_1-\theta_2)-s(2\theta_1+\theta_2) \\ 2s(2\theta_2)+s(2(\theta_1-\theta_2))-s(2(\theta_1+\theta_2)) \\ 3s(\theta_1-\theta_2)-3s(\theta_1+\theta_2)-s(\theta_1-3\theta_2)+s(\theta_1+3\theta_2) \end{bmatrix} \quad (30)$$

$$Det[SD]=\begin{bmatrix} l^2 r_{P2}^2 c(\zeta_{P2}^2) \\ r_{B2}^2 r_{P2}^2 s(\zeta_{B2}^2)(\zeta_{P2}^2) \\ r_{B2}^2 r_{P2}^2 s(\zeta_{B2}) c(\zeta_{B2}) c(\zeta_{P2}^2) \\ l r_{B2} r_{P2}^2 c(\zeta_{B2}^2) c(\zeta_{P2}^2) \\ -l r_{B2} r_{P2}^2 c(\zeta_{B2}) c(\zeta_{P2}^2) \end{bmatrix}^T \begin{bmatrix} c(\theta_5)+0.5c(2\theta_4-\theta_5)+0.5c(2\theta_4+\theta_5) \\ c(\theta_5)-0.5c(2\theta_4-\theta_5)-0.5c(2\theta_4+\theta_5) \\ -c(\theta_4)+0.5c(\theta_4-2\theta_5)+0.5c(\theta_4+2\theta_5) \\ -s(\theta_4)+0.5s(\theta_4-2\theta_5)+0.5s(\theta_4+2\theta_5) \\ s(2\theta_4-\theta_5)+s(2\theta_4+\theta_5) \end{bmatrix} \quad (31)$$

5. Conclusion

This paper computes the workspace of the DPM, which is decoupled into a positional workspace generated by the first PM and an orientational workspace generated by the second PM. For each workspace, the singularities are analytically examined by the Jacobian matrix transforming the velocity of each platform to those of the linear actuators. The Jacobian is decoupled to a central axis, the first PM and the second PM, each is separately analyzed to find singularity points with rank deficiency. No singularity in the central axis occurs but those in the first and the second PM arise with distinct loci when the combined angles of θ_i(i=1, 2) or θ_i(i= 4, 5) are close to $\pm 90°$ regardless of θ_3.

This indicates that the singularities arise outside the regular workspace. Therefore, it is concluded that the DPM is free from the singularity problem inside its regular workspace.

Acknowledgement

This research was financed by the Korea Science & Engineering Foundation(KOSEF 981-1001-006-1).

References

Fichter. E. F., 1986, "A Stewart Platform-Based Manipulator: General Theory and Practical Construction", *J. of Rob. Res.*, Vol. 5, pp. 157~182.

Gosselin, C., 1990, "Determination of the Workspace of 6-dof Parallel Manipulators", *J. of Mech. and Design*, pp. 331~336.

Gosselin, C. and Angeles, J., 1990, "Singularity Analysis of Closed-Loop Kinematic Chains," *IEEE J. Robotics and Auto.*, Vol. 6, No. 3, pp. 281~290.

Gosselin, C. M., Perreault, L. and Vaillancourt, C., 1995, "Simulation and Computer aided Kinematic Design of Three-Degree-of-Freedom Spherical parallel Manipulator," *J. of Rob. Sys.*

12(12), pp. 857~869,

Kerr, D. R, 1989, "Analysis, Properties, and Design of a Stewart Platform Transducer," *J. of Mech., Trans. , and Auto. in Design*, Vol. 111, pp. 25~28,

Kreyszig, E. 1983, *Advanced Engineering Mathematics*, Wiley, New York, pp. 439~447.

Lee, M. K., 1995 "Design of a High Stiffness Machining Robot Arm Using Double Parallel Mechanism," *IEEE Conf. Rob. and Auto.*, Nagoya, pp. 234~240.

Lee, M. K. and Park, K. W. , 1997, "Real Time Direct Kinematics of a Double Parallel Manipulator," *J. of KSME*, Vol. 21 No. 1, pp. 144~153.

Long, G. L. and Collins, C. L. , 1995, "The Singularity Analysis of an In-Parallel Hand Controller for Force-Reflected Teleoperation," *IEEE J. of Rob. and Auto.* vol. 11, no. 5, pp. 661~669.

Merlet, J. 1994, "Trajectory Verification in the workspace for Parallel Manipulators," *J. of Rob. Res.*, Vol. 13, No. 4, pp. 326~333.

Sugimoto, K., 1987, "Kinematic and Dynamic Analysis of Parallel Manipulators by Means of Motor Algebra," *ASME J. of Mech. Trans. and Auto. in Design*, Vol. 109, pp. 3~7.

Waldron, K. J., Raghavan, M. and Roth, B., 1989, "Kinematics of a Hybrid Series Parallel Manipulator System," *ASME J. of Dyn. Sys., Meas. and Cont.*, Vol. 111, pp. 211~221.